Chemical Physics 482 (2017) 221–225

Contents lists available at ScienceDirect

Chemical Physics

journal homepage: www.elsevier.com/locate/chemphys

# Interatomic Coulombic Decay of HeNe dimers after ionization and excitation of He and Ne

H. Sann [a], T. Havermeier [a], H.-K. Kim [a], F. Sturm [a], F. Trinter [a], M. Waitz [a], S. Zeller [a], B. Ulrich [a], M. Meckel [a], S. Voss [a], T. Bauer [a], D. Schneider [a], H. Schmidt-Böcking [a], R. Wallauer [b], M. Schöffler [a], J.B. Williams [c], R. Dörner [a], T. Jahnke [a,*]

[a] Institut für Kernphysik, Universität Frankfurt, Max-von-Laue-Str. 1, 60438 Frankfurt, Germany
[b] Fachbereich Physik, Philipps-Universität Marburg, Renthof 5, 35032 Marburg, Germany
[c] Department of Physics, Reno University, NV 89557, USA

ARTICLE INFO

*Article history:*
Available online 7 September 2016

ABSTRACT

We study the decay of a helium/neon dimer after ionization and simultaneous excitation of either the neon or the helium atom using Cold Target Recoil Ion Momentum Spectroscopy (COLTRIMS). We find that, depending on the decaying state, either direct Interatomic Coulombic Decay (ICD) (i.e. mediated by a virtual photon exchange), exchange ICD (mediated by electron exchange) or radiative charge transfer occurs. The corresponding channels are identified.

© 2016 Elsevier B.V. All rights reserved.

## 1. Introduction

After the prediction of Interatomic Coulombic Decay (ICD) in 1997 by Cederbaum and coworkers [1] it was found that this electronic decay process involving two or more atoms or molecules of a loosely bound compound of matter is a very common phenomenon [2]. As ICD occurs, an electronic excitation of one atom or molecule decays by a transfer of the excitation energy to a different, neighboring atom or molecule. It was experimentally confirmed in the early 2000s by three pioneering experiments employing electron spectroscopy [3], Cold Target Recoil Ion Momentum Spectroscopy [4] and the lifetime analysis of photoelectron spectra [5]. ICD has been found since then in a manifold of atomic and molecular systems and different excitation schemes [2,6].

ICD of HeNe mixed dimers has been studied already about 6 years ago by Sisourat et al. [7]. Intriguingly, it turned out, that in case of Ne(2*s*) shake-up ionization it is the nuclear motion that dominates the Interatomic Coulombic Decay. Depending on the exact state populated, Sisourat and coworkers identified, that ICD may only occur after the dimer stretches to rather large internuclear distances of up to 7 Å, as the decay is energetically forbidden for smaller internuclear distances. Accordingly, a drastic increase of the decay width was observed to occur with the periodicity of the vibrational motion of the dimer's nuclei. In the present article we give a comprehensive overview over all ICD channels following photoionization of HeNe and identify all decaying states and decay processes involved after shake-up ionization of either the Ne or the He atom. The decay rate of ICD can be described theoretically (in the lowest pertubation order) by the electron/electron-Coulomb-matrix element. In the *prototype case* of ICD (i.e. ICD after Ne(2*s*) innervalence ionization) the decay rate is proportional to $|V_{L2p,R2p,L2s,k} - V_{L2p,R2p,k,L2s}|^2$, where the two contributions to the overall matrix element

$$V_{L2p,R2p,L2s,k} = \iint \phi^*_{L2p}(\vec{r}_1)\phi_{L2s}(\vec{r}_1)\frac{e^2}{|\vec{r}_1-\vec{r}_2|} \phi^*_{R2p}(\vec{r}_2)\phi_k(\vec{r}_2)d\vec{r}_1 d\vec{r}_2 \quad (1)$$

and

$$V_{L2p,R2p,k,L2s} = \iint \phi^*_{L2p}(\vec{r}_1)\phi_k(\vec{r}_1)\frac{e^2}{|\vec{r}_1-\vec{r}_2|} \phi^*_{R2p}(\vec{r}_2)\phi_{L2s}(\vec{r}_2)d\vec{r}_1 d\vec{r}_2 \quad (2)$$

are referred to as *direct* and *exchange* contribution in the literature [8,9]. *L2s* and *L2p* denote the 2*s* and 2*p* orbitals located at the *left* atom and *R2p* denotes the 2*p* orbital situated at the *right* atom.

In direct ICD the excited valence electron fills the vacant hole in its own atom. In the case of exchange ICD the electron, which fills the hole, comes from the atom that did not have the initial vacancy. Fig. 1 shows a sketch of both contributions to the ICD matrix element. The resulting electrons and ions are indistinguishable, but the processes depend very differently on the internuclear distance *R*. As exchange ICD requires an overlap of the electron and hole orbitals both located at different atoms its probability increases with smaller internuclear distances.

* Corresponding author.
*E-mail address:* jahnke@atom.uni-frankfurt.de (T. Jahnke).

http://dx.doi.org/10.1016/j.chemphys.2016.09.008
0301-0104/© 2016 Elsevier B.V. All rights reserved.

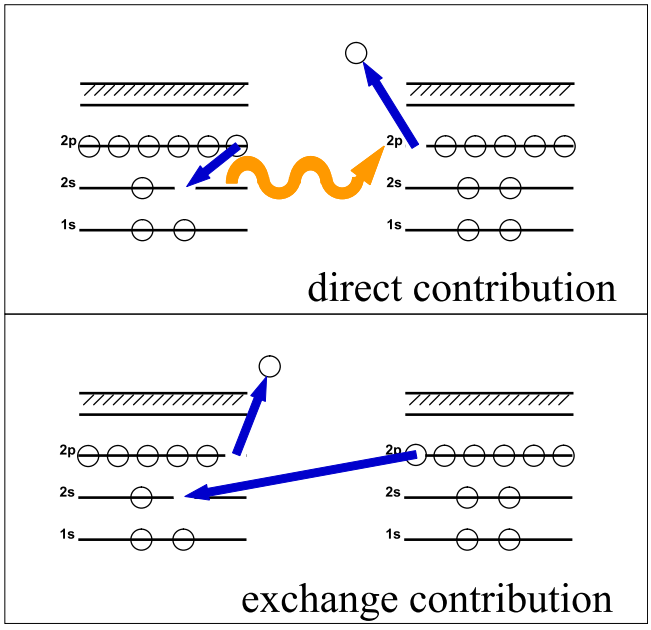


**Fig. 1.** Sketch of the direct contribution (top) and the exchange contribution (bottom) to the ICD transition matrix element as ICD in a neon dimer occurs after inner valence ionization.

In 2007 Jahnke et al. demonstrated that these contributions can be disentangled in an experiment due to the *R*-dependence of their probability [10]. The experimental data presented in this article shows similar signatures of *direct* and *exchange* ICD depending on the parity of the decaying shake-up states.

## 2. Experimental technique

The experiment was performed at the BESSY synchrotron radiation source at beamline U125-2_SGM in single bunch operation using the COLTRIMS technique [11–13]. A supersonic gas jet containing 93% He and 7% Ne was expanded through a nozzle of 20 μm diameter and then intersected with a linearly polarized photon beam. The gas jet was precooled to 40 K to create helium/-neon mixed dimers. The ions and electrons were guided by homogeneous electric and magnetic fields towards two position and time sensitive microchannel plate detectors with delay line readout [14]. The electron arm of the spectrometer employed McLaren time focusing [15] with an overall length of 6.8 cm, while the ion arm consisted solely of an homogeneous acceleration region of a length of 2.4 cm. From their times-of-flight and positions of impact we obtained the momentum vectors and thus the energy of all charged reaction fragments in coincidence. The two singly charged ions in the final state are emitted back-to-back with equal momentum. Accordingly, by requiring a zero sum momentum of the two measured ions we were able to distinguish the HeNe dimers from the vast amount of monomer background. Additionally, due to the coincidence measurement we were able to distinguish $Ne_2$ dimers, which are also created in the expansion, from HeNe dimers. Two measurements were conducted. The first one at a photon energy of $h\nu = 55.8$ eV, below the threshold to create $He^{+*}(n = 2)$ and a second one at $h\nu = 72.4$ eV, i.e. above that threshold. The field strengths of the spectrometer were 5.2 V/cm and 0.5 mT for the first measurement and 8.9 V/cm and 0.7 mT for the second one.

## 3. Results – A. ICD after Ne(2*s*) shake-up

ICD in the HeNe dimer can either be induced by exciting the neon atom or the helium atom. As mentioned in the introduction, the former was investigated already in an earlier work by Sisourat et al. [7]. There it was shown that the contribution to ICD of the decay of the $He–Ne^+(2s^{-1})$ state is very small because the dimer needs to stretch before ICD becomes energetically possible and instead the main contribution comes from $He–Ne^+(2p^{-2}3s)$ shake-up states. Here we show that, additionally, there is a significant contribution from the decay of the $He–Ne^+(2p^{-2}3p)$ shake-up states. The transition from $Ne^+(2p^{-2}3p)$ to the ICD final state $Ne^+(2p^{-1})$ is dipole forbidden. Therefore, the decay rate via *direct ICD* is very small as a decay of that kind is dominated by a dipole transition due to the virtual photon exchange [17]. Instead *exchange ICD* may occur. In earlier work by Jahnke et al. on shake-up ICD of $Ne_2$ dimers the two contributions were disentangled experimentally by investigating the kinetic energy release (KER) of the two ions after the decay (and the subsequent Coulomb explosion). Within the reflection approximation [16] the kinetic energy release is a direct measure of the internuclear distance of the dimer's atoms at the instant of the decay. At the large internuclear distances of interest the potential energy curves of the repulsive doubly charged states are in good approximation $\sim 1/R$. Therefore, in atomic units, the internuclear distance $R$ is obtained as $R = 1/KER$. The decay probability of the two contributions scales differently with the internuclear distance of the two atoms involved in the decay: while the direct ICD is dominated by a dipole/dipole-interaction and thus scales with $1/R^6$ [17,18], the exchange ICD depends on an orbital overlap of the contributing electron and hole states. Its probability decreases exponentially with increasing $R$. Accordingly, the two contributions occur within different KER ranges, namely direct ICD at smaller KER values (as it occurs at larger internuclear distances) and exchange ICD after the dimer contracted significantly (as compared to its ground state mean internuclear distance) and thus after establishing a sufficient amount of orbital overlap. Fig. 2 shows the corresponding results. We identify two groups of kinetic energy releases. Small KER values correspond to a decay at large internuclear distance (pathways A1–A4), close to the equilibrium distance of the neutral HeNe. These events result from direct ICD. The group of events at larger KERs (B1, B2) result from electron exchange ICD.

In Fig. 2 we plot the measured energy of either of the two electrons emitted during the process. Horizontal features of a constant, KER-independent, electron energy indicate a photoelectron, while diagonal lines for which the sum of the KER and the electron energy is constant depict measured ICD electrons. This allows to identify the corresponding states (see Table 1). The direct ICD contributions occur in a range of 1.5 eV < KER < 5 eV. This correlates to a range of internuclear distances of 2.9 Å to 9.6 Å. A1 marks the decay of $He–Ne^+(2s^{-1})$. A2 and A3 mark decays of the $2p^{-2}3s$ shake up states with symmetry $^3P$ and $^1D$ [19,20]. The energy positions can be found in Table 1. The notations used are the ones for the atomic states in the dissociation limit. In our earlier work by Sisourat et al. [7] the corresponding molecular terms were employed. Accordingly, the A1 state corresponds to a molecular state with $^2\Sigma^+$ symmetry. For A2 there are two corresponding molecular states with $^2\Sigma^-$ and $^2\Pi$ symmetry and for A3 the corresponding molecular state has $^2\Sigma^+$ symmetry.

In addition to the ICD electrons the corresponding photoelectrons are visible, as well, in Fig. 2. The photoelectrons belonging to states A1 and A2 (see Fig. 2) occur at 7.3 eV and 6.3 eV, respectively. In this energy range a structure occurs which rather resembles a tilted line than two separated peaks. As mentioned above, a tilted line is a typical fingerprint for an ICD electron. If this feature stems from an ICD electron its corresponding photoelectron is expected to have close to zero kinetic energy. This fits well to a decay of the $He–Ne(2p^{-2}3s)$ state where the Ne has $^1S$ symmetry in the atomic limit (labeled as A4) [19]. Accordingly, the ICD events

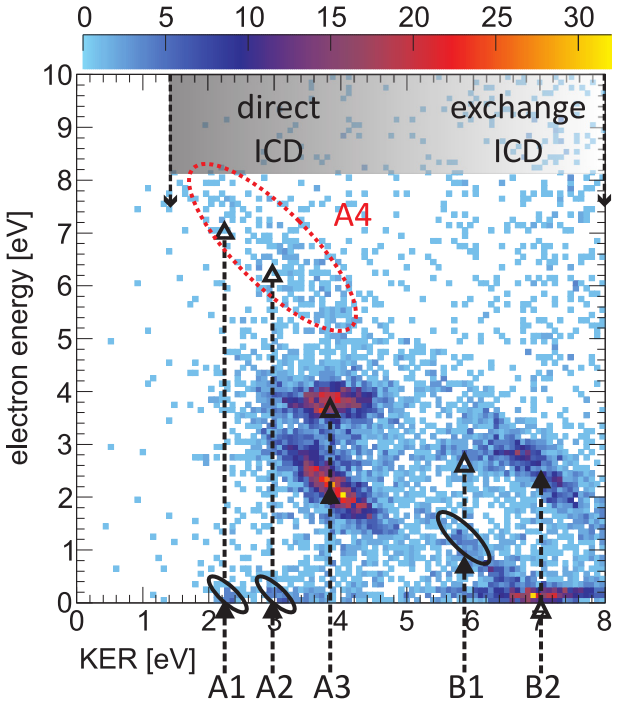


**Fig. 2.** The experimental yield is plotted as a function of the kinetic energy release of the doubly ionized HeNe dimer and the kinetic energy of the measured electrons. The measurement was performed at a photon energy of $h\nu$ = 55.8 eV, ~7 eV above the Ne($2s^{-1}$) threshold. The different ICD channels A1, A2, A3, B1, B2 are given in Table 1. The open arrowheads indicate the positions of the photoelectrons and the full arrowheads the location of ICD electrons. The two regions of KER, which correspond to the different processes (direct and exchange ICD), are indicated as well.

from decays of the states A1 and A2 seem to overlap with photoelectrons from the decay of this $^1$S state (area within the red ellipse in Fig. 2).

In the range of larger KER values (i.e. 5.5 eV < KER < 8 eV) the contributions of exchange ICD are observable. The KER values correspond to internuclear distances from 1.8 Å to 2.6 Å. The two visible decay pathways are labeled as B1 and B2 in the figure and correspond to decays of the $^3$P and $^1$D states of He–Ne$^+$($2p^{-2}3p$) [19].

The relative intensities of the different contributions are extracted from the experimental data and shown in Table 1. When comparing the obtained ratios to those measured in experiments on Ne monomers [19] the relative intensities extracted from the dimer data differ strongly. The reason for that behavior in case of direct ICD has been depicted in [7]: the Franck–Condon overlap of the low lying excited states is very small (as it is only present for very large internuclear distances) and accordingly the highest shake-up state (A3) is predominantly populated. A similar effect could be responsible for the relative population ratios of the states that undergo exchange ICD, but corresponding potential energy curves to verify this assumption are not available in the literature.

## 4. Results – B. ICD after He(1*s*) shake-up

A second measurement was conducted at $h\nu$ = 72.4 eV. At this energy it is possible to ionize one electron of the He atom and excite the other electron to the He$^{+*}$($n$ = 2) state. In earlier work on resonant ICD in HeNe Trinter et al. resonantly excited the He atom of the dimer to the He($1s3p$) state and investigated the occurrence of HeNe$^+$ ions in dependence of the photon energy used for the excitation [21,22]. The shake-up ionization examined here is energetic enough to allow for the emission of a total of two electrons. Fig. 3 shows the corresponding coincidence map of KER vs. electron energy for the case of a breakup of the dimer into He$^+$/N$^+$ in the final state. Even though the processes described in the previous section are obviously energetically allowed as well, at these higher photon energies, it turns out that the shake-up ionization of the He atom and a subsequent ICD leading to the ionization of the Ne atom is the dominant ICD pathway. The photoelectron appears at an energy of 7 eV and its corresponding ICD electron can be found along a diagonal line belonging to a constant sum kinetic energy of the ions and the ICD electron. The corresponding relative intensities are also given in Table 1.

Fig. 4 shows the kinetic energy release occurring due to ICD after He$^+$($n$ = 2)-shake-up ionization comparing it to the well-known kinetic energy release distribution obtained for the same excitation channel in the case of a He dimer [23]. In the previous section the KER was employed to differentiate the direct from the exchange contribution to the IC decay. This approach relies on the fact, that the ICD due to the direct term is very efficient and thus occurring close to the mean internuclear distance of the dimer ground state (and thus resulting in small KER values). If the overall ICD efficiency is too low, this differentiation is no longer possible, as the contributions from both terms mix due to the nuclear dynamics occurring prior to the decay. In that case a very common, more general picture is helpful, in which the KER simply images the vibrational wave packet of the excited state prior to ICD [24,25]. Comparing the KER distributions obtained for $He_2$ and HeNe within this picture, distinct differences, as well as similarities, can be found: firstly, the overall width of the KER distribution is similar. This might seem surprising at first glance, as the helium dimer is known to be a hugely extended system with a mean internuclear distance of approx. 50 Å [26]. However, the excited and ionized state is much more tightly bound and has accordingly a much smaller mean internuclear distance because of the strong polarization induced by the singly charged He atom. As ICD in the helium dimer occurs on a comparably long timescale, the mean internuclear distance contributing to ICD is mainly dominated by the smaller internuclear distances existing for the singly charged and excited dimer. Secondly, the HeNe KER does not show sharp

**Table 1**
The different states contributing to ICD after absorption of a photon of $h\nu$ = 55.8 eV or $h\nu$ = 72.4 eV. The relative intensities are extracted from the experimental data depicted in Fig. 2 and Fig. 3. Additionally, the regions of KER and photoelectron energies $E_\gamma$ are given.

| State | Configuration | Decay type | KER [eV] | $h\nu$ = 55.8 eV | | $h\nu$ = 72.4 eV | |
|---|---|---|---|---|---|---|---|
| | | | | $E_\gamma$ [eV] | Rel. intensity | $E_\gamma$ [eV] | Rel. intensity |
| A1 | Ne($2s^{-1}$) | Direct | 2 | 7.3 | <5% | 23.9 | <5% |
| A2 | Ne($2s^22p^43s$) $^3$**P** | Direct | 3 | 6.3 | <5% | 22.9 | <5% |
| A3 | Ne($2s^22p^43s$) $^1$**D** | Direct | 2.8–4.5 | 3.8 | 65% | 20.4 | 15% |
| A4 | Ne($2s^22p^43s$) $^3$**P** | Direct | 2–4 | 0 | <5% | 16.6 | <5% |
| B1 | Ne($2s^22p^43p$) $^3$**P** | Exchange | 5.5–6.5 | 2.8 | <5% | 19.4 | <5% |
| B2 | Ne($2s^22p^43p$) $^1$**D** | Exchange | 6–8 | 0 | 30% | 16.6 | 20% |
| He $n$ = 2 | He$^{+*}$($n$ = 2) | – | 3–9 | – | – | 7 | 60% |

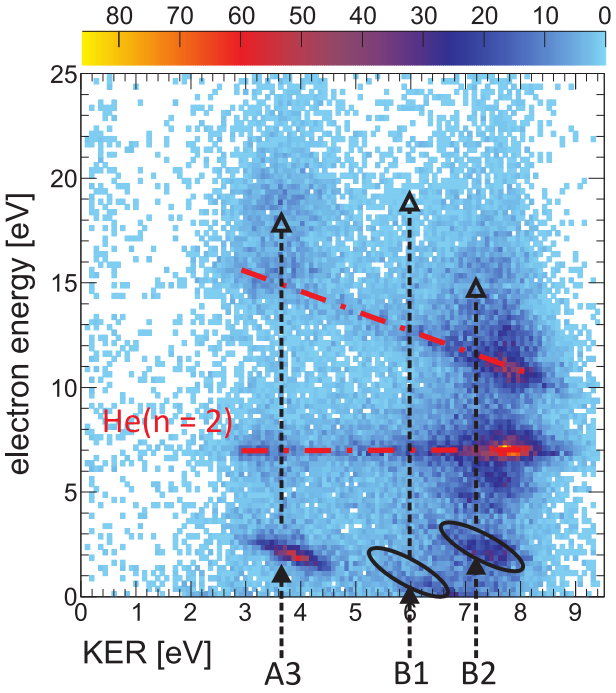


**Fig. 3.** The experimental yield is plotted as a function of the kinetic energy release and the energy of the electron for a measurement at $h\nu = 72.4$ eV, 7 eV above the $He^+(n = 2)$ threshold. The photoelectron and the ICD electron corresponding to ICD after excitation of the He atom are indicated by dash-dotted lines. The open arrowheads indicate the positions of the photoelectrons and the full arrowheads the location of ICD electrons. The other structures belong to the two most probable IC decays after excitation of the Ne atom which have been discussed in Section 3.

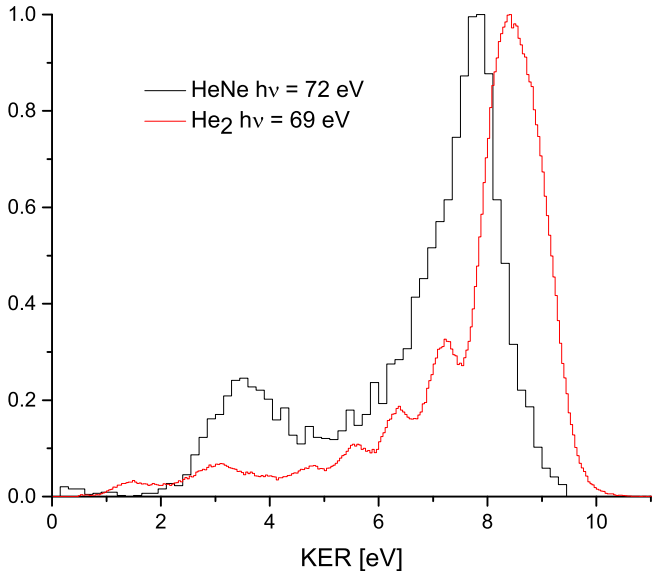


**Fig. 4.** The kinetic energy release of the HeNe dimer (black line) and $He_2$ (red line) after excitation of a helium atom to the $He^{+*}(n = 2)$ state and subsequent ICD. (For interpretation of the references to colour in this figure caption, the reader is referred to the web version of this article.)

vibrational features, which are observable in $He_2$. In $He_2$ they result from high-lying vibrational states which are populated due to the Franck–Condon overlap with the very delocalized neutral ground state. Time-resolved studies of ICD in $He_2$ [27] showed that these features build up during longer decay times.

In Fig. 5 the total kinetic energy of all reaction fragments (i.e. the kinetic energy of the two ions, the photoelectron $e^-_\gamma$ and the

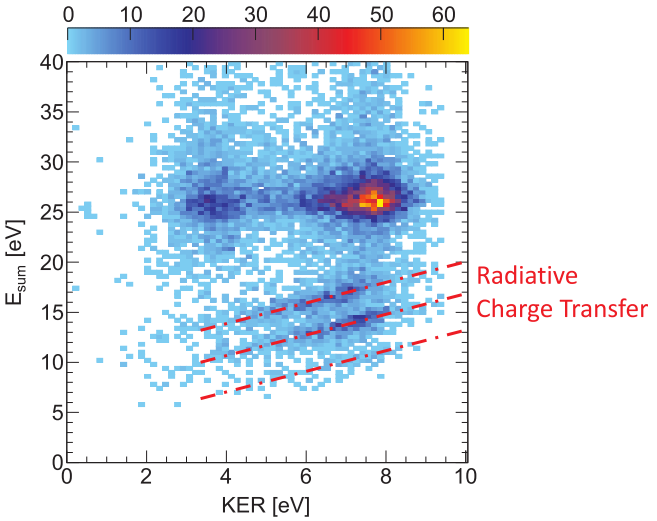


**Fig. 5.** The experimental yield is plotted as a function of the sum kinetic energy of all charged particles occurring after the photoreaction ($Ne^+$ $He^+$, $e^-_\gamma$, $e^-_{ICD}$) and the kinetic energy release. The three structures identified as radiative charge transfer are indicated by red dotted-dashed lines. (For interpretation of the references to colour in this figure caption, the reader is referred to the web version of this article.)

ICD electron $e^-_{ICD}$) is plotted against the KER. As the different ICD process pathways all result in the same final state of $He^+(1s^{-1})$–$Ne^+(2p^{-1})$ the kinetic energy sum has to be the same for all cases. Its value can be calculated by subtracting the ionization potentials of neon and helium from the photon energy employed:

$$E_{sum} = h\nu - IP_{Ne} - IP_{He} = 72.4\ \text{eV} - 21.56\ \text{eV} - 24.59\ \text{eV} = 26.25\ \text{eV} \quad (3)$$

Fig. 5 shows indeed a horizontal line at a sum energy of approx. 26 eV. Additionally, however, three more tilted lines occur at lower energies. As these lines refer to cases where a certain amount of the total energy is missing and as that amount depends on the value of the KER, the underlying process can be identified as a radiative charge transfer (RCT) where a photon carried away a certain portion of the total energy. In this process the Ne atom is doubly ionized in the first step. In a second step the charge is distributed by the emission of a photon. The three tilted lines visible belong to different doubly ionized $Ne^{2+}$ states, not only occupying the lowest lying state of $Ne^{2+}(2p^{-2})$, which has $^3P$ symmetry in the atomic limit, but also the two other $2p^{-2}$ states, which have $^1D$ and $^1S$ symmetry.

## 5. Conclusion

We reported on a comprehensive study of ICD in HeNe mixed dimers after shake-up ionization of either the Ne or the He atom of the dimer. Similar to previous results on shake-up induced ICD (SICD) in $Ne_2$ [10] two distinct regions of kinetic energy releases are populated depending on the parity of the decaying state. This is due to the fact, that either direct or exchange ICD takes place: If the parity of the decaying state is *even* a decay mediated by the emission of a virtual photon is allowed (i.e. a dipole allowed decay) and the decay occurs close to typical internuclear distances of the ground state of the dimer. If, however, the decaying state is of *odd* parity, only exchange ICD is possible. Due to the need of orbital overlap for these cases of ICD, the measured kinetic energy release is increased, i.e. the dimer decays after substantially contracting to much smaller internuclear distances. Additionally, several occurrences of radiative charge transfer have been

observed and assigned after shake-up ionization of the He atom of the dimer.

## Acknowledgement

Acknowledgement This work was supported by the DFG as a part of the DFG-Forschergruppe FOR1789. We would like to acknowledge the great collaborative work within this research unit and are grateful for many discussions and lots of inspiration for experiments provided by K. Gokhberg, A. Kuleff, N. Sisourat and L.S. Cederbaum. We would like to thank U. Hergenhahn and K. Ueda for outstanding collaboration during the last decade. The great support by the staff of the BESSY synchrotron is acknowledged. Happy birthday, Lenz!

## References

[1] L.S. Cederbaum, J. Zobeley, F. Tarantelli, Phys. Rev. Lett. 79 (1997) 4778.
[2] T. Jahnke, J. Phys. B: At. Mol. Opt. Phys. 48 (2015) 082001.
[3] S. Marburger, O. Kugeler, U. Hergenhahn, T. Möller, Phys. Rev. Lett. 90 (2003) 203401.
[4] T. Jahnke, A. Czasch, M.S. Schöffler, S. Schössler, A. Knapp, M. Käsz, J. Titze, C. Wimmer, K. Kreidi, R.E. Grisenti, A. Staudte, O. Jagutzki, U. Hergenhahn, H. Schmidt-Böcking, R. Dörner, Phys. Rev. Lett. 93 (2004) 163401.
[5] G. Öhrwall, M. Tchaplyguine, M. Lundwall, R. Feifel, H. Bergersen, T. Rander, A. Lindblad, J. Schulz, S. Peredkov, S. Barth, S. Marburger, U. Hergenhahn, S. Svensson, O. Björneholm, Phys. Rev. Lett. 93 (2004) 173401.
[6] U. Hergenhahn, J. Electron Spectrosc. Relat. Phenom. 184 (2011) 78.
[7] N. Sisourat, H. Sann, N.V. Kryzhevoi, P. Kolorenč, T. Havermeier, F. Sturm, T. Jahnke, H.-K. Kim, R. Dörner, L.S. Cederbaum, Phys. Rev. Lett. 105 (2010) 173401.
[8] R. Santra, J. Zobeley, L.S. Cederbaum, Phys. Rev. B 64 (2001) 245104.
[9] R. Santra, L.S. Cederbaum, Phys. Rep. 368 (2002) 1.
[10] T. Jahnke, A. Czasch, M. Schöffler, S. Schössler, M. Käsz, J. Titze, K. Kreidi, R.E. Grisenti, A. Staudte, O. Jagutzki, L. Schmidt, T. Weber, H. Schmidt-Böcking, K. Ueda, R. Dörner, Phys. Rev. Lett. 99 (2007) 153401.
[11] R. Dörner, V. Mergel, O. Jagutzki, L. Spielberger, J. Ullrich, R. Moshammer, H. Schmidt-Böcking, Phys. Rep. 330 (2000) 95.
[12] J. Ullrich, R. Moshammer, A. Dorn, R. Dörner, L.P.H. Schmidt, H. Schmidt-Böcking, Rep. Prog. Phys. 66 (2003) 1463.
[13] T. Jahnke, T. Weber, T. Osipov, A.L. Landers, O. Jagutzki, L.P.H. Schmidt, C.L. Cocke, M.H. Prior, H. Schmidt-Böcking, R. Dörner, J. Electron. Spectrosc. Relat. Phenom. 141 (2004) 229.
[14] O. Jagutzki, A. Cerezo, A. Czasch, R. Dorner, M. Hattas, V. Mergel, U. Spillmann, K. Ullmann-Pfleger, T. Weber, H. Schmidt-Bocking, G. Smith, IEEE Trans. Nucl. Sci. 49 (2002) 2477.
[15] W.C. Wiley, I.H. McLaren, Rev. Sci. Instrum. 26 (1955) 1150.
[16] E.A. Gislason, J. Chem. Phys. 58 (2001) 3702.
[17] V. Averbukh, I.B. Müller, L.S. Cederbaum, Phys. Rev. Lett. 93 (2004) 263002.
[18] V. Averbukh, L.S. Cederbaum, J. Chem. Phys. 123 (2005) 204107.
[19] G. Kutluk, T. Takaku, M. Kanno, T. Nagata, E. Shigemasa, A. Yagishita, F. Koike, J. Phys. B: At. Mol. Opt. Phys. 27 (1994) 5637.
[20] A.E. Kramida, G. Nave, Eur. Phys. J. D 39 (2006) 331.
[21] F. Trinter, J.B. Williams, M. Weller, M. Waitz, M. Pitzer, J. Voigtsberger, C. Schober, G. Kastirke, C. Müller, C. Goihl, P. Burzynski, F. Wiegandt, R. Wallauer, A. Kalinin, L. Schmidt, M. Schöffler, Y.-C. Chiang, K. Gokhberg, T. Jahnke, R. Dörner, Phys. Rev. Lett. 111 (2013) 233004.
[22] G. Jabbari, S. Klaiman, Y.-C. Chiang, F. Trinter, T. Jahnke, K. Gokhberg, J. Chem. Phys. 140 (2014) 224305.
[23] T. Havermeier, T. Jahnke, K. Kreidi, R. Wallauer, S. Voss, M. Schöffler, S. Schössler, L. Foucar, N. Neumann, J. Titze, H. Sann, M. Kühnel, J. Voigtsberger, J. H. Morilla, W. Schöllkopf, H. Schmidt-Böcking, R.E. Grisenti, R. Dörner, Phys. Rev. Lett. 104 (2010) 133401.
[24] S. Scheit, L.S. Cederbaum, H.-D. Meyer, J. Chem. Phys. 118 (2003) 2092.
[25] N. Sisourat, N.V. Kryzhevoi, P. Kolorenc, S. Scheit, T. Jahnke, L.S. Cederbaum, Nat. Phys. 6 (2010) 508.
[26] R.E. Grisenti, W. Schöllkopf, J.P. Toennies, G.C. Hegerfeldt, T. Köhler, M. Stoll, Phys. Rev. Lett. 85 (2000) 2284.
[27] F. Trinter, J.B. Williams, M. Weller, M. Waitz, M. Pitzer, J. Voigtsberger, C. Schober, G. Kastirke, C. Müller, C. Goihl, P. Burzynski, F. Wiegandt, T. Bauer, R. Wallauer, H. Sann, A. Kalinin, L. Schmidt, M. Schöffler, N. Sisourat, T. Jahnke, Phys. Rev. Lett. 111 (2013) 093401.